

Dynamical Self-Quenching of Spin Pumping into Double Quantum Dots

Arne Brataas¹ and Emmanuel I. Rashba²

Department of Physics, Norwegian University of Science and Technology, NO-7491 Trondheim, Norway
Department of Physics, Harvard University, Cambridge, Massachusetts 02138, USA

Nuclear spin polarization can be pumped into spin-blocked quantum dots by multiple Landau-Zener passages through singlet-triplet anticrossings. By numerical simulations of realistic systems with 10^7 nuclear spins during 10^5 sweeps, we uncover a mechanism of dynamical self-quenching which results in a fast saturation of the nuclear polarization under stationary pumping. This is caused by screening the random field of the nuclear spins. For moderate spin-orbit coupling, self-quenching persists but its patterns are modified. Our finding explains low polarization levels achieved experimentally and calls for developing new protocols that break the self-quenching limitations.

PACS numbers: 73.63.Kv, 72.25.Pn, 76.70.Fz

Double quantum dots (DQDs) are promising platforms for spintronics [1] and quantum computing [2–5]. For qubits encoded in singlet (S) and triplet (T) states of spin blockaded DQDs [6], the hyperfine coupling of electron spins to the nuclear spin reservoir is critical. Although electron spin relaxation caused by this coupling is destructive, a properly controlled nuclear polarization is an efficient tool for performing rotations of S - T_0 qubits [7, 8]; T_0 is the zero component of the electron spin triplet (T_0, T_{\pm}). A widely discussed approach for pumping nuclear spin polarization into a DQD is based on multiple Landau-Zener (LZ) passages across the $S - T_+$ anticrossing [9–13] (T_+ is the lowest energy component of the triplet T in GaAs). In the absence of spin-orbit (SO) coupling, angular momentum conservation requires that each transformation of the S state into the T_+ state is accompanied by the net transfer of one quantum unit of angular momentum to the nuclear subsystem. Multiple $S \rightarrow T_+$ passages increase the nuclear spin polarization, but experimental data show that spin pumping typically saturates at a surprisingly low level of about 1% [14], and the origin of this puzzling behavior remains unknown. Higher levels of the nuclear polarization differences (“gradients”) between the two dots were only achieved by using feedback loop schemes [15].

In this Letter, we show that nuclear spin pumping produces dynamical screening of *both* the SO coupling and the random hyperfine (Overhauser) field controlling the width of the $S - T_+$ anticrossing as well as the efficiency of spin pumping, while the detailed patterns differ. The screening results in one of the nuclear spin configurations with a vanishing anticrossing width, $v \rightarrow 0$. Hence, the probability of the $S \rightarrow T_+$ transition and the angular momentum transfer inevitably vanish, resulting in quenching of spin pumping. We call this *dynamical self-quenching* of spin pumping into double quantum dots borrowing the word “self-” from the theory of polarons, where self-trapping implies a joint evolution of the electron and phonon subsystems [16].

As applied to hyperfine coupled systems, this conclusion appears to agree with the concept of dark states en-

visioned in Ref. [17] and further discussed in Ref. [10]; the latter paper is mostly concerned with the building of gradient fields. However, the existence of dark states has no direct experimental confirmation yet. On the theoretical side, the patterns of highly-nonlinear coupled electron-nuclear dynamics that might bring systems including millions of nuclear spins into such states remain unclear. To resolve the problem, we performed large scale numerical simulations for realistic systems. Our procedure (i) evaluates the coherent precession of the coupled electron spin and about 10^7 nuclear spins subject to an external magnetic field during a large number (up to 10^5) of LZ sweeps through the $S - T_+$ anticrossing and (ii) computes the building of the nuclear polarization during each LZ sweep. The calculations unveiled the gross features of the self-quenching process. Among our results, the following are of special importance: (i) self-quenching sets in under generic conditions, (ii) spin-orbit interaction is dynamically screened despite the violation of the angular momentum conservation, (iii) durations of $S - T_+$ pulses have a critical effect on the quenching dynamics, and (iv) dynamical screening is robust with respect to moderate noise levels.

We consider two electrons in a double quantum dot that can be in singlet or triplet states and represent the orbital part of the wave function as $\psi_S(\mathbf{r}_1, \mathbf{r}_2)$ or $\psi_T(\mathbf{r}_1, \mathbf{r}_2)$. The electrons are coupled to the nuclear spins via the hyperfine coupling Hamiltonian

$$H_{hf} = V_s \sum_{\lambda} A_{\lambda} \sum_{j \in \lambda} \sum_{m=1,2} \mathbf{I}_{j\lambda} \cdot \mathbf{s}(m) \delta(\mathbf{R}_{j\lambda} - \mathbf{r}_m), \quad (1)$$

where $\mathbf{s}(m) = \boldsymbol{\sigma}(m)/2$ are the electron spin operators in terms of the Pauli matrices $\boldsymbol{\sigma}$, $m = 1, 2$ enumerates electrons, \mathbf{r}_m are electron coordinates, $\mathbf{I}_{j\lambda}$ are nuclear spins, λ enumerates nuclear species and j lattice sites $\mathbf{R}_{j\lambda}$, A_{λ} are hyperfine coupling constants for the species λ , and V_s is a volume per unit cell. We consider GaAs that has three spin $I = 3/2$ nuclear species ^{69}Ga , ^{71}Ga , and ^{75}As . All GaAs parameter values are known [5, 18, 19] and listed in Ref. [20]. The electrons and nuclear spins are subject to an external magnetic field which is

aligned along the z -direction.

Before presenting our numerical results, we review how electronic Landau-Zener sweeps influence nuclear spins [13]. The hyperfine interaction of Eq. (1) couples two electrons to a large number of nuclear spins. We account for the effect of this interaction by using a semi-classical Born-Oppenheimer approach so that the slow nuclear spins produce a coupling between the singlet and triplet electronic states. In turn, the nuclear spins are driven by the electron dynamics controlled by time-dependent gate voltage variations. The variations causing Landau-Zener transitions occur in the interval $-T_{\text{LZ}} \leq t \leq T_{\text{LZ}}$ and they are repeated many times after waiting for a time T_w , where $T_w \gg T_{\text{LZ}}$. During the waiting time T_w , the nuclear spins are only affected by the external magnetic field and not by the electrons. During the LZ sweeps, the voltage changes also induce relative shifts of the electron singlet and triplet energy levels driving passages of the system through the $S-T_+$ anti-crossing, Fig. 1(a). Restricting the discussion to its vicinity and disregarding contributions of the (T_0, T_-) spectrum branches, the coupled equations for singlet and triplet amplitudes $c_S(t)$ and $c_{T_+}(t)$ are ($\hbar = 1$)

$$i\partial_t \begin{pmatrix} c_S \\ c_{T_+} \end{pmatrix} = \begin{pmatrix} \epsilon_S & v^+ \\ v^- & \epsilon_{T_+} - \eta \end{pmatrix} \begin{pmatrix} c_S \\ c_{T_+} \end{pmatrix}, \quad (2)$$

where $\epsilon_S(t)$ and $\epsilon_{T_+}(t)$ are electronic energies controlled by the gates. The off-diagonal matrix elements of Eq. (2), $v^\pm = v_n^\pm + v_{\text{so}}^\pm$, include contributions from the nuclear spins generated by the hyperfine coupling

$$v_n^\pm = V_s \sum_\lambda A_\lambda \sum_{j \in \lambda} \rho_{j\lambda} (I_{j\lambda}^x \pm iI_{j\lambda}^y) / \sqrt{2} \quad (3)$$

and from the spin-orbit coupling v_{so}^\pm [21]. The diagonal contribution $\eta = \eta_Z + \eta_n$ includes the Zeeman energy of the T_+ state in the external magnetic field $\mathbf{B} = B\hat{\mathbf{z}}$ and the Overhauser field of the nuclear polarization, $\eta_n = -V_s \sum_\lambda A_\lambda \sum_{j \in \lambda} \zeta_{j\lambda} I_{j\lambda}^z$ which is defined solely by the coupling of the triplet component of the electron wave function to the longitudinal nuclear spin polarization. The singlet-triplet coupling constants are $\rho_{j\lambda} = \int d\mathbf{r} \psi_S^*(\mathbf{r}, \mathbf{R}_{j\lambda}) \psi_T(\mathbf{r}, \mathbf{R}_{j\lambda})$ and the coupling constants in the T_+ state are $\zeta_{j\lambda} = \int d\mathbf{r} |\psi_T(\mathbf{r}, \mathbf{R}_{j\lambda})|^2$.

Between the Landau-Zener cycles, during every waiting period of duration T_w , the nuclear spins precess in the external magnetic field. It is assumed that the time-scale T_{LZ} for the LZ transition (induced by rapid changes in the gate voltages) is much shorter than the nuclear precession times t_{pr} for the species in the external magnetic field, $t_{71\text{As}}$, $t_{69\text{Ga}}$, and $t_{71\text{Ga}}$, respectively. Because of the large number of nuclei in the dot, $N \sim 10^6 - 10^7$, the changes $\Delta \mathbf{I}_{j\lambda}$ acquired by individual spins during a single sweep are minor. We evaluate them by integrating the equations of coherent nuclear dynamics $d\mathbf{I}_j/dt = \mathbf{\Delta}_j \times \mathbf{I}_j$ over the Landau-Zener transition time $-T_{\text{LZ}} \leq t \leq T_{\text{LZ}}$.

Here $\mathbf{\Delta}_j$ are the Knight fields following from Eq. (1). Finally, $\Delta \mathbf{I}_{j\lambda} = \mathbf{\Gamma}_{j\lambda} \times \mathbf{I}_{j\lambda}$, where

$$\Gamma_{j\lambda}^{(x)} = -V_s A_\lambda \rho_{j\lambda} (Pv_y + Qv_x) / (2v^2), \quad (4a)$$

$$\Gamma_{j\lambda}^{(y)} = V_s A_\lambda \rho_{j\lambda} (Pv_x - Qv_y) / (2v^2), \quad (4b)$$

$$\Gamma_{j\lambda}^z = V_s A_\lambda \zeta_{j\lambda} R / (2v), \quad (4c)$$

with $v = |v^\pm| = \sqrt{(v_x^2 + v_y^2)/2}$ and $v^\pm = (v_x \pm iv_y) / \sqrt{2}$. In these expressions, $0 \leq P \leq 1$ is the $S-T_+$ transition probability and an unbounded real number Q is the shake-up parameter defined as [13]

$$P + iQ = -i2v^- \int_{-T_{\text{LZ}}}^{T_{\text{LZ}}} dt c_S(t) c_{T_+}^*(t) \quad (5)$$

in terms of the singlet (triplet) amplitudes, and $R = 2v \int_{-T_{\text{LZ}}}^{T_{\text{LZ}}} dt |c_{T_+}(t)|^2$ accounts for the Knight shift due to the electron spin in the triplet T_+ state during the Landau-Zener transition.

It follows from Eq. 2 and Eq. 5 that P is equal to the change of the occupation of the singlet state $|c_S(t)|^2$ during the sweep and therefore coincides with the LZ transition probability. The change ΔI_z in the total longitudinal magnetization I_z equals

$$\Delta I_z = -\frac{P}{2v^2} (v^- v_n^+ + v^+ v_n^-) - i\frac{Q}{2v^2} (v^- v_n^+ - v^+ v_n^-). \quad (6)$$

When $v_{\text{so}}^\pm = 0$, the second term in Eq. 6 vanishes and $\Delta I_z = -P$ as required by the conservation of the angular momentum. In the same scenario, $Q \neq 0$ and describes the angular momentum transfer inside the DQD due to the shakeup processes induced by the LZ pulses [13]. When $v_{\text{so}}^\pm \neq 0$, Q also mediates the angular momentum leakage from the DQD due to the spin-orbit coupling. Because the integral for P converges fast at the scale of $t \sim 1/|v^\pm|$ while the integral for Q diverges as $\ln T_{\text{LZ}}$ for linear LZ sweeps, Q is typically large, especially for $P \approx 1$, and deeply influences the self-quenching process.

Using the amplitudes $(c_S(t), c_{T_+}(t))$ found from solving Eq. (2) in combination with the dynamical equations for nuclear spins of Eq. (4) makes our approach completely self-consistent. During a single LZ sweep, $\epsilon_S(t)$ and $\epsilon_{T_+}(t)$ change fast while staying close to the anti-crossing, and η and v^\pm remain practically constant. The singlet wave function of the DQD in the $S-T_+$ anticrossing point can be expressed as $\psi_S = \cos \nu \psi_{02} + \sin \nu \psi_{11}$, where ψ_{02} and ψ_{11} are the singlet wave functions with both electrons on the right dot and two electrons equally distributed between the dots, respectively. The mixing angle ν is controlled by B and detuning and was chosen as $\nu = \pi/4$.

Our simulations included about 10^7 nuclei up to those with a hyperfine interaction strength of only 1% of the

maximum one, which allowed us to account for the electronic density heterogeneity and the spin polarization transfer from the interior to the periphery. Our algorithm allowed performing calculations for different T_{LZ} with the identical initial distribution.

For each sweep, the DQD is first set in its eigenstate at $t = -T_{LZ}$ that is close, but not identical, to the singlet (0,2) state with both electrons localized at the right dot. Then a change in the gate voltages drives a (partial) transition to the triplet (1,1) state with electrons shared between both dots. Finally the electronic system is reset in its initial state. We assume that the LZ transition time T_{LZ} are much shorter than the nuclear precession times t_{pr} and compute the change in the direction of each of the nuclear spins during every sweep numerically, as described by Eqs. (2)-(5). Between consecutive sweeps, repeated with a period of the waiting time T_w , electrons are in the singlet state and do not interact with the nuclear spins that coherently precess in the external field. We choose realistic parameters for a parabolic DQD of a height $w = 3$ nm, size $\ell = 50$ nm, and interdot separation $d = 100$ nm; magnetic field $B = 10$ mT. All the results presented below were found for the same initial configuration of nuclear spins, but we have checked that they are representative for generic initial configurations.

For the shape of the $S \rightarrow T_+$ pulses, we used the LZ model with $\epsilon_s(t) = \epsilon_{\max}t/2T_{LZ}$ and $\epsilon_{T_+} - \eta = -(\epsilon_{\max}t/2T_{LZ}) - (\eta - \eta_i)$, where η_i is the initial polarization $\eta_i = \eta(t = -T_{LZ})$ and $\epsilon_{\max} = 2.5$ meV, which is larger than the typical S - T_+ coupling. To avoid trivial quenching due to the shift in η caused by the accumulating polarization, the electronic energies were renormalized after every 100 sweeps to keep $\eta - \eta_i \approx 0$. As a result, the center of the sweep was permanently kept close to the anticrossing point. Such a regime can be achieved experimentally by applying appropriate feedback loops. SO coupling in DQDs is device specific, and in GaAs it changes from weak to moderate, so we consider it both in the limit of no SO coupling [7, 22] and with SO coupling of a reasonable magnitude [23, 24].

Fig. 1(b) plots the change in the total nuclear polarization, ΔI_z , as a function of the number of sweeps n , for $v_{so} = 0$ and four transition times T_{LZ} ; the difference in the parameter values of all three nuclear species is taken into account. The evolution of ΔI_z typically saturates within 3×10^4 sweeps. The saturation proves the self-quenching of the transverse nuclear polarizations that controls the singlet-triplet coupling v_n^\pm shown in Fig. 1(c). It vanishes after a number of LZ transitions and this typically happens faster for longer LZ durations T_{LZ} (a larger transition probability), but more complicated patterns of subsequent revivals of the v_n^\pm can also be seen. Volatile dynamics of v_n^\pm seen in Fig. 1(c), with multiple maxima and minima, is typical of multi-species systems because of the different spin precession rates of different species. However, finally the nuclear subsystem self-

synchronizes in one of the states in which it decouples from the electron spin qubit, and this is our first *central result*. The contribution of each of the species to v_n^\pm vanishes identically, at each instant; $v_n^\pm = 0$ persists even after the LZ pumping is interrupted (not shown). This result resembles the “dark states” of Refs. 10, 17.

With $N \sim 10^6$ nuclei in the DQD, the initial fluctuations producing v_n^\pm is $N^{1/2} \sim 10^3$. For $P \sim 1$, one expects that at least $n \sim 10^3$ pulses are needed for balancing it. The typical number of pulses to establish self-quenching of about $n \sim 10^4$ of Fig. 1(b) is one order of magnitude larger, which can be attributed to the high volatility of the process and the fact that the LZ probability P in each cycle is less than one.

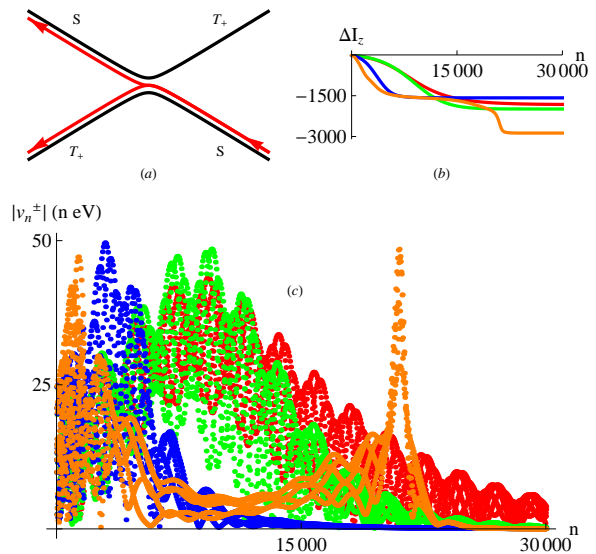


FIG. 1: Nuclear dynamics in absence of SO coupling as a function of sweep number n ; difference in the parameters of the three nuclear species is taken into account. Resonant waiting time $T_w = t_{75As} = 13.7\mu s$; qualitative pattern do not depend on this specific choice. (a) Landau-Zener passage of a singlet S through a S - T_+ anticrossing. Energy levels (black) and evolution of S into entangled S and T_+ states (red). (b) Change in the nuclear spin polarization ΔI_z and (c) hyperfine-induced singlet-triplet coupling $|v_n^\pm|$. Color codes: $T_{LZ} = 10$ ns (red), 20 ns (green), 40 ns (blue), and 80 ns (orange).

Next, we consider the effect of the SO coupling. To illustrate the main qualitative result, we ascribe to all nuclei identical parameters found by averaging over the three GaAs species [20] and consider strictly resonant pumping, $T_w = t_{GaAs} = 10.7\mu s$, t_{GaAs} being the nuclear precession time [25]. We use realistic values of the SO coupling, $v_{so} = 0, 31,$ and 62 neV [26] (and choose it to be a real number). The LZ transition probability shown in Fig. 2(a) vanishes at large n , hence, the pumping is self-quenched also in this case. At this point, it is crucial to note that all our numerical results for v_n^\pm and ΔI_z are plotted at multiples of the waiting time

T_w . Hence, self-quenching in a resonant ($T_w = t_{\text{GaAs}}$) SO coupled system is achieved through $v_n^\pm \rightarrow -v_{\text{so}}$ ($v^\pm = v_n^\pm + v_{\text{so}}^\pm$) at every multiple of the Larmor period, and nuclear polarization screens the SO coupling, Fig. 2. This screening of SO coupling is our next *central result*. However, in contrast to the case of no SO coupling, between the sweeps (not shown), the matrix elements $v_n^\pm(t)$ change harmonically with the amplitude v_{so} and a period t_{GaAs} , $v_n \rightarrow v_{\text{so}} \cos(2\pi t/t_{\text{GaAs}})$, where the time $t = nT_w = nt_{\text{GaAs}}$ at the LZ sweep number n . Not surprisingly, while $|v_n^\pm|$ reaches its T_{LZ} -independent limit, the change in the polarization, ΔI_z , depends on T_{LZ} . Fig. 2(a) shows that P is large, $P \sim 1$, and fluctuates fast with n . The mechanism of fast dynamics is unveiled by the high magnitude of the shakeup parameter $Q \sim 20 \gg 1$. While P describes pure injection of the angular momentum, Q describes its redistribution due to shakeup processes and the SO coupling [13]. Remarkably, it is seen from Eq. (6) that the effect of the Q term on ΔI_z vanishes in two important limits, when $v_{\text{so}} = 0$ and $v_n^\pm = -v_{\text{so}}$. Fig. 3(c) demonstrates that self-quenching sets in sharply for large T_{LZ} , and the fluctuational phase lasts longer for larger v_{so} values; v_n^\pm always saturate at $-v_{\text{so}}$. For SO coupled systems, the change ΔI_z in the magnetization is non-monotonic in n and shows no regular dependence on v_{so} , Fig. 2(d).

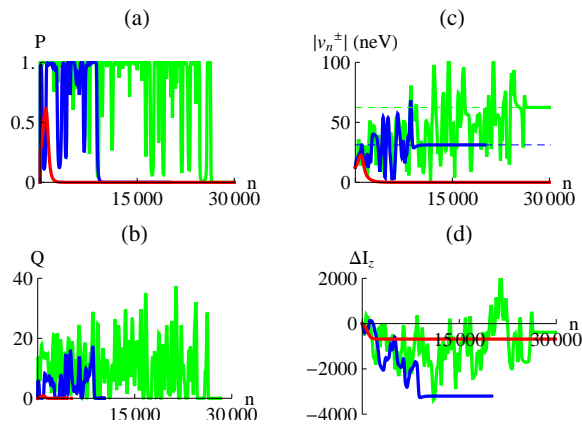


FIG. 2:

Nuclear dynamics for variable spin-orbit coupling v_{so} driven by long pulses $T_{\text{LZ}} = 160$ ns; single-specie model with $T_w = t_{\text{GaAs}}$. (a) Landau-Zener probability P , (b) shakeup parameter Q , (c) hyperfine-induced singlet-triplet coupling $|v_n^\pm|$, and (d) change ΔI_z in the total nuclear polarization; in (c), dashed lines mark spin-orbit coupling. Color codes: $v_{\text{so}} = 0$ (red), 31 neV (blue), and 62 neV (green).

To test how robust our results are, we modeled the influence of noise by adding a random magnetic field along the z -direction for each nuclear spin so that the nuclear spins acquire an additional phase of $2\pi r_{j\lambda} T_w / \tau$ during each waiting time between LZ sweeps, where $r_{j\lambda}$ are random numbers in the interval from -1 to 1; τ is the noise correlation time (see Ref. [20]) for more details).

Fig. 3 demonstrates the effect of the noise that randomizes the phases of the precessing nuclear spins. It displays the magnitude of the hyperfine matrix element v_n^\pm at every multiple of the waiting time T_w for no noise and for two noise levels. In all cases, v_n^\pm approaches the value $\approx -v_{\text{so}}$ at $n \lesssim 50000$. While in the absence of the noise the saturation of v_n^\pm is exact at all multiples of the waiting time T_w , $v_n^\pm = -v_{\text{so}}$ (blue curve), noisy systems experience slight fluctuations near this value, see especially the red line which only saturates at $n \approx 5 \times 10^4$. We conclude that for moderate noise levels, the dynamical screening is robust, and this is our final *central result*.

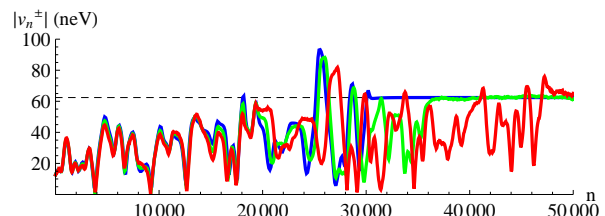


FIG. 3: Effect of noise on nuclear dynamics. The LZ sweep duration of $T_{\text{LZ}} = 80$ ns; single-specie model with $T_w = t_{\text{GaAs}}$. Hyperfine-induced singlet-triplet coupling $|v_n^\pm|$ for spin-orbit coupling $v_{\text{so}} = 62$ neV and increasing levels of transverse noise. Black dashed lines show SO coupling. Color codes: $\tau/t_{\text{GaAs}} = \infty$ (blue), 5000 (green), and 2500 (red); t_{GaAs} is the nuclear spin precession time and τ is the noise correlation time.

The above results prove that dynamical self-quenching is a rather generic property of the GaAs type DQDs pumped by multiple passages through the $S - T_+$ anticrossing [27]. In a quenched state, the electron spin qubit becomes screened from the randomness of the nuclear spin bath, and therefore its decoherence by nuclei [28–30] is expected to be suppressed; trapping the qubit into the quenched state can be checked by spin splitter technique [31, 32]. A quenched qubit can be operated by short pulses applied to the gates due to the different dependence of v_n^\pm and v_{so} on the shape of the electron wave functions. This subject requires further consideration.

In conclusion, self-quenched states produced by stationary pumping of a spin blockaded double quantum dot by multiple passages through the $S - T_+$ anticrossing decouples the electronic qubit from the nuclear spin bath. In such states the dynamical nuclear polarization screens both the initial random Overhauser field and a moderate spin orbit coupling typical of GaAs quantum dots. Self-quenching unveils the origin of the low spin pumping efficiency encountered in experimental studies.

A. B. would like to thank B. I. Halperin for his hospitality at Harvard University where this work was initiated. E. I. R. acknowledges funding from the Intelligence Advanced Research Project Activity (IARPA) through the Army Research Office.

-
- [1] I. Žutić, J. Fabian, and S. Das Sarma, *Rev. Mod. Phys.* **76** 323 (2004)
- [2] D. Loss and D. P. DiVincenzo, *Phys. Rev. A* **57**, 120 (1998).
- [3] J. Levy, *Phys. Rev. Lett.* **89**, 147902 (2002).
- [4] *Semiconductor Spintronics and Quantum Computation*, ed. by D. D. Awschalom, D. Loss, and N. Samarth (Springer, Berlin), 2002.
- [5] R. Hanson, L. P. Kouwenhoven, J. R. Petta, S. Tarucha, and L. M. K. Vandersypen, *Rev. Mod. Phys.* **70**, 1217 (2007).
- [6] K. Ono, D. G. Austing, Y. Tokura, and S. Tarucha, *Science* **297**, 1313 (2002).
- [7] J. R. Petta, A. C. Johnson, J. M. Taylor, E. A. Laird, A. Yacoby, M. D. Lukin, C. M. Marcus, M. P. Hanson, and A. C. Gossard, *Science* **309**, 2180 (2005).
- [8] M. D. Shulman, O. E. Dial, S. P. Harvey, H. Bluhm, V. Umansky, and A. Yacoby, *Science* **336**, 202 (2012).
- [9] G. Ramon and X. Hu, *Phys. Rev. B* **75**, 161301(R) (2007).
- [10] M. Gullans, J. J. Krich, J. M. Taylor, H. Bluhm, B. I. Halperin, C. M. Marcus, M. Stopa, A. Yacoby, and M. D. Lukin, *Phys. Rev. Lett.* **104**, 226807 (2010).
- [11] M. S. Rudner, I. Neder, L. S. Levitov, and B. I. Halperin, *Phys. Rev. B* **82**, 041311 (2010).
- [12] H. Ribeiro and G. Burkard, *Phys. Rev. Lett.* **102**, 216802 (2009).
- [13] A. Brataas and E. I. Rashba, *Phys. Rev. B* **84**, 045301 (2011).
- [14] D. J. Reilly, J. M. Taylor, J. R. Petta, C. M. Marcus, M. P. Hanson, and A. C. Gossard, *Phys. Rev. Lett.* **104**, 236802 (2010).
- [15] H. Bluhm, S. Foletti, D. Mahalu, V. Umansky, and A. Yacoby, *Phys. Rev. Lett.* **105**, 216803 (2010).
- [16] *Polarons in Advanced Materials*, ed. by A. S. Alexandrov (Canopus, Bristol, UK), 2007.
- [17] J. M. Taylor, A. Imamoglu, and M. D. Lukin, *Phys. Rev. Lett* **91**, 246802 (2003).
- [18] J. Schliemann, A. Khaetskii, and D. Loss, *J. Phys. Condens. Matter* **15**, R1809 (2003).
- [19] J. M. Taylor, J. R. Petta, A. C. Johnson, A. Yacoby, C. M. Marcus, and M. D. Lukin, *Phys. Rev. B* **76**, 035315 (2007).
- [20] See supplementary material at EPAPS.
- [21] M. S. Rudner and L. S. Levitov, *Phys. Rev. B* **82**, 155418 (2010).
- [22] R. Brunner, Y.-S. Shin, T. Obata, M. Pioro-Ladriere, T. Kubo, K. Yoshida, T. Taniyama, Y. Tokura, and S. Tarucha, *Phys. Rev. Lett.* **107**, 146801 (2011).
- [23] S. D. Ganichev, V. V. Belkov, L. E. Golub, E. L. Ivchenko, P. Schneider, S. Giglberger, J. Eroms, J. De Boeck, G. Borghs, W. Wegscheider, D. Weiss, and W. Prettl, *Phys. Rev. Lett.* **92**, 256601 (2004).
- [24] K. C. Nowack, F. H. L. Koppens, Yu. V. Nazarov, L. M. K. Vandersypen, *Science* **318**, 1430 (2007).
- [25] Multi-specie SO coupled systems require a generalized description [33].
- [26] Estimated similarly to Ref. [34].
- [27] While non-resonant pumping of SO coupled DQDs produces more complexities, spin pumping remains at a low level.
- [28] W. Yao, R.-B. Liu, and L. J. Sham, *Phys. Rev.* **74**, 195301 (2006).
- [29] L. Cywiński, W. M. Witzel, and S. Das Sarma, *Phys. Rev. Lett.* **102**, 057601 (2009).
- [30] J. Fisher and D. Loss, *Science* **324**, 1277 (2009).
- [31] J. R. Petta, H. Lu, A. C. Gossard, *Science* **327**, 669 (2010).
- [32] H. Ribeiro, J. R. Petta, and G. Burkard, *Phys. Rev. B* **82**, 115445 (2010).
- [33] A. Brataas and E. I. Rashba, unpublished.
- [34] C. Fasth, A. Fuhrer, L. Samuelson, V. N. Golovach, and D. Loss, *Phys. Rev. Lett.* **98**, 266801 (2007).

EPAPS SUPPLEMENTARY MATERIAL FOR "DYNAMICAL SELF-QUENCHING OF SPIN PUMPING INTO DOUBLE QUANTUM DOTS"

In this supplementary, we provide details of the parameters used in the numerical calculations, describe the effective single-specie model, show how nuclear spins precess in an external magnetic field between Landau-Zener sweeps, and discuss the noise model.

Parameters

GaAs has 8 nuclear spins per cubic unit cell so that the effective volume per site is $V_s = a^3/8$, where the lattice constant is $a = 5.65\text{\AA}$. When all nuclear spins are fully polarized, the Overhauser field seen by the electrons is 5.3 T. The electron g -factor is $g_{\text{GaAs}} = -0.44$. The other parameters reflecting the abundance, g -factors, and hyperfine coupling constants are listed in Table I.

	69Ga	71Ga	75As
p	30%	20%	50%
g	1.3	1.7	0.96
A (μeV)	77	99	94
I	3/2	3/2	3/2

TABLE I: Nuclear abundances p , nuclear g -factors, hyperfine coupling constants A , and nuclear spin in GaAs.

Effective Single-Specie Model

To illustrate the main qualitative effects of SO coupling, we also make use of an effective single-specie model. In the effective single-specie model, the mean nuclear g -factor is $g_{\text{GaAs}} = \sum_{\lambda} p_{\lambda} g_{\lambda} = 1.21$, the mean hyperfine coupling constant is $A_{\text{GaAs}} = \sum_{\lambda} p_{\lambda} A_{\lambda} = 90\mu\text{eV}$, and the mean nuclear spin is $I_{\text{GaAs}} = \sum_{\lambda} p_{\lambda} I_{\lambda} = 3/2$.

Nuclear Precession in the External Magnetic Field

Landau-Zener sweeps of a duration T_{LZ} are repeated with wait periods of T_{w} long compared with T_{LZ} , hence, $T_{\text{LZ}} \ll T_{\text{w}}$. Between consecutive Landau-Zener sweeps, electrons are in the singlet state and do not interact with the nuclear spins. However, during the waiting interval T_{w} , nuclear spins precess in an external magnetic field B applied along the z -direction. Then, the coherent evolution of the nuclear spins are

$$I_{j\lambda}^x(t + T_{\text{w}}) = I_{j\lambda}^x(t) + I_{j\lambda}^x(t) \cos \phi_{j\lambda} - I_{j\lambda}^y(t) \sin \phi_{j\lambda}, \quad (7a)$$

$$I_{j\lambda}^y(t + T_{\text{w}}) = I_{j\lambda}^y(t) + I_{j\lambda}^y(t) \cos \phi_{j\lambda} + I_{j\lambda}^x(t) \sin \phi_{j\lambda}, \quad (7b)$$

$$I_{j\lambda}^z(t + T_{\text{w}}) = I_{j\lambda}^z(t), \quad (7c)$$

where t is the initial time of the interval, the transverse phase change is $\phi_{j\lambda} = -2\pi T_{\text{w}}/t_{\lambda}$ in terms of the spin precession time $t_{\lambda} = 2\pi\hbar/g_{\lambda}\mu_I B$, $g_{\lambda} = \mu_{\lambda}/I_{\lambda}$ is the g -factor for a nuclear specie λ , μ_{λ} its magnetic moment and $\mu_I = 3.15 \times 10^{-8}$ eV/T is the nuclear magneton.

Noise

We neglected in our calculations the effects of the magnetic dipole-dipole interaction between the nuclear spins that is slow at our time scale and also the possible electrical noise on the gates. The detailed study of these effects is beyond the scope of our paper.

We use a simple model to consider the influence of such noise by phenomenologically adding a random magnetic field along the z -direction for each *individual* nuclear spin so that the accumulated phase in Eq. 7 changes, $\phi_{j\lambda} \rightarrow \phi_{j\lambda}^{\text{eff}} = \phi_{j\lambda} + \phi_{j\lambda}^{\text{noise}} = -2\pi T_{\text{w}}(1/t_{\lambda} - r_{j\lambda}/\tau)$, where $r_{j\lambda}$ are random numbers in the interval from -1 to 1 for each

nuclear spin. This procedure simulates a randomization of the transverse components of the nuclear spins after a time of the order τ , and τ is termed the noise correlation time.

Quantitatively, the noise averages of the phase-dependent factors in Eq. 7 become

$$\frac{1}{2} \int_{-1}^1 dr \cos \phi_{j\lambda}^{\text{eff}} = \cos \phi_{j\lambda} \frac{\sin(2\pi T_w/\tau)}{2\pi T_w/\tau}, \quad (8)$$

$$\frac{1}{2} \int_{-1}^1 dr \sin \phi_{j\lambda}^{\text{eff}} = \sin \phi_{j\lambda} \frac{\sin(2\pi T_w/\tau)}{2\pi T_w/\tau}, \quad (9)$$

so that the phase-coherent information contained in the transverse nuclear spins components are lost after a time of the order of the noise correlation time τ . By introducing noise, any possible build-up of the matrix elements v_n^\pm is therefore lost after a time of the order of the noise correlation time τ .
